J. Fluid Mech. (1981), *vol.* 111, *pp.* 421–437
Printed in Great Britain

Velocity field in a steady breaker

By J. A. BATTJES

Department of Civil Engineering, Delft University of Technology, Delft, The Netherlands

AND T. SAKAI

Department of Civil Engineering, Kyoto University, Kyoto, Japan

(Received 14 September 1980 and in revised form 5 February 1981)

An experimental investigation is described of the velocity field in a steady, spilling-type breaker, generated on a steady current by a submerged hydrofoil. Velocities have been measured with a laser–doppler system, and analysed with respect to mean and r.m.s. values as well as Reynolds stresses. The results indicate that the turbulent flow field downstream of the initiation of the separation at the surface resembles that in a self-similar turbulent wake.

1. Introduction

The process of wave breaking on a beach is fundamental to many coastal engineering problems. The loss of organized wave energy leads to the generation of nearshore currents and to turbulence, which are key factors in the mechanics of sediment motion and in the processes of nearshore transport and mixing in general, while knowledge of the remaining wave energy is important with respect to the wave attack on shore structures.

Despite its practical importance, systematic knowledge of the velocity field in breaking waves, either empirical or theoretical, is very scarce. A lack of proper instrumentation has considerably hindered the acquisition of good experimental data, while the turbulent and aerated flow does not easily lend itself to theoretical approaches.

Longuet-Higgins & Turner (1974) have developed a model for a spilling breaker. They consider a turbulent, aerated surface roller, emanating from a wave crest, and riding down the inclined face of the main body of the wave, in which the flow is laminar. Air entrainment into the surface roller is accounted for, as well as entrainment of mass and momentum across the interface between roller and wave.

Peregrine & Svendsen (1978) have proposed a model for the flow field in a class of steady and quasi-steady breaking flows such as hydraulic jumps, bores and spilling breakers. They concluded from visual observations that the turbulent flow, immediately following the breaking, resembles a turbulent mixing layer, which arises because the smooth flow from upstream meets the relatively slowly moving water in the toe of a surface roller. This roller, which is small compared with the region of high-intensity turbulence, it is believed does not play an important role in the dynamics of the wave, other than triggering the turbulence.

In Peregrine & Svendsen's model, the region of turbulent flow following breaking is supposed to spread downstream and downward as in a mixing layer; at some

distance downstream the upper region becomes affected by gravity, and for waves in shallow water the lower region becomes affected by the bottom. Still further downstream there is a so-called wake or decay region.

In the context of spilling breakers on a beach, it seems plausible that Longuet-Higgins & Turner's model may be applicable to the initial stages of the wave breaking, which is inherently unsteady, and that of Peregrine & Svendsen to the later stage, in which a quasi-uniform, quasi-steady bore has developed. We have concentrated on the latter stage and have therefore considered Peregrine & Svendsen's model only.

The usefulness of a model such as this is that it enables one to describe the main features of the turbulence induced by breaking in terms of better known classes of turbulent flows. However, the model is partly hypothetical. It is based on visual observations, which are largely qualitative. A more quantitative verification is still needed. It is the purpose of the present study to contribute to such verification, through the measurement and analysis of the mean flow, the turbulent intensities, the turbulent shear stresses, and their decay with distance downward and downstream†.

The contents of the paper are as follows. The experimental arrangement and procedure are described first. This is followed by a presentation and discussion of the main results. It is concluded that at a distance of a few breaker heights downstream of the initial breaking, the flow appears to have become self-similar. Its principal parameters vary with downstream distance as in a turbulent wake.

2. Experimental arrangement and procedures

2.1. *Flow conditions*

The experiments described in the following were performed in a wave-current flume of the Laboratory of Fluid Mechanics, Department of Civil Engineering, Delft University of Technology. Its length is approximately 33 m and its width 0·80 m. The flume bottom is horizontal. The side walls consist of glass panels, supported by vertical steel columns 1·5 m apart.

As stated in the introduction, the purpose of the present study is to investigate the turbulence induced by a breaking water surface, with special reference to the model proposed by Peregrine & Svendsen (1978) for the flow field in a class of steady or quasi-steady breakers. A partial check of the validity of that model can be obtained in a breaker in which the mean (non-turbulent) motion is steady.

A classical case of a steady breaking flow is the hydraulic jump. There have been measurements of mean velocity and turbulence in hydraulic jumps (see, for example, Resch & Leutheusser, 1972; Resch, Leutheusser & Coantic 1976). However, as pointed out by Peregrine & Svendsen, these were for strong jumps only. Such flows are not directly relevant to breakers on a beach, in which we are ultimately interested. Another difference between these two categories is that the flow in a jump even in the upper regions is greatly influenced by the boundary-layer development in the upstream, supercritical flow, as shown by Resch & Leutheusser (1972). We do not expect that this is the case for the flow in periodic or quasi-periodic bores on a beach, because of the oscillatory character of the latter.

† After completion of this study, results of a similar investigation were reported by Stive (1980), whose conclusions closely parallel ours.

The preceding considerations have led us to the choice of a steady breaker which should be relatively unaffected by a bottom boundary layer, and the geometry of which should resemble that of a spilling breaker or a post-breaking bore on a beach. We have created such a flow condition by inserting a hydrofoil below the free surface of a steady flow in a laboratory flume.

Since in our experiment the breaking was induced artificially by the hydrofoil section, there is no need for the entire upstream flow to be supercritical, or even to have a Froude number near 1. We could therefore choose a relatively large depth (larger than the critical depth for the given maximum discharge), so as to obtain an extensive region in which the post-breaking turbulent flow near the free surface would not be affected by the proximity of the bottom. All measurements were performed with a mean depth (h) of 0·58 m in the uniform flow upstream of the hydrofoil.

It is commonly observed that the breaking of an air–water interface on a small scale, as in a typical laboratory experiment, gives rise to less air entrainment than it does on a larger scale, typical of field conditions. However, there is no consensus concerning the importance of this for the overall dynamical similarity between the motions on the two scales. Führböter (1970) attaches much significance to a proper scaling of the air entrainment for the study of breaking waves. On the other hand, Peregrine & Svendsen (1978) point out that without air entrainment the motion can be very turbulent 'with all the other qualitative characteristics of a breaking'. They suggest in fact, for experimental reasons, to carry out measurements in breaking waves on such a small scale that air entrainment is avoided entirely.

We did not want merely to *assume* Froude similarity. For that reason we have carried out the main series of measurements at maximum discharge, so as to minimize possible scale effects. This experiment will be referred to as 'full scale'. In addition, some measurements were made at a reduced scale, so as to obtain insight into the nature and magnitude of possible scale effects.

A hydrofoil section was chosen with a relatively full profile, i.e. a rather slow decrease of thickness from the cross section of maximum thickness to the trailing edge, so as to produce a correspondingly full profile of low pressure along its upper surface at moderate angles of attack. A NACA 6024 profile (Abbott & Von Doenhoff 1949) was used. The hydrofoil spanned effectively the entire flume width. In the preliminary runs (see below), it was supported from above, through the free surface. In the actual experiments, it was mounted between two thin (1 mm) metal plates which were held flat against the glass panels; these plates in turn were attached to the flume bottom so that there were no obstacles in the flume above the level of the hydrofoil, and only minor ones below it. The mounting of the hydrofoil permitted variations of its depth of submergence and of the angle of attack with respect to the upstream flow.

Preliminary runs were made, using a hydrofoil with 20·0 cm chord and 4·8 cm maximum thickness, in which the depth of the centre of the hydrofoil below the undisturbed mean water level (d) and the downward angle of the chord from the horizontal (α) were varied, in order to find conditions which appeared suitable to our purpose. Photographs were made of the flow, in which the free surface and the extent of air entrapment were visible, as well as the dispersion of dye injected upstream. For the values of mean depth and discharge mentioned above, useable flows were obtained for values of d from about 0·15 m to 0·30 m, and for values of α from about 5° to 20°.

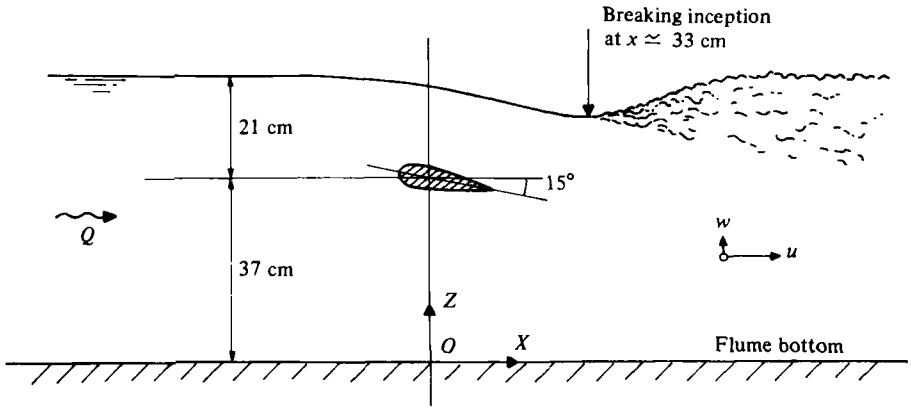

FIGURE 1. Sketch indicating flow condition and definition of reference frame.

Run	h (m)	U (m s^{-1})	c (cm)	Δ (cm)	d (cm)	α (deg)
Full scale	0·58	1·08	20·0	4·8	21·0	15
Half scale	0·58	0·66	10·0	2·4	10·5	15

TABLE 1. Independent experimental variables.

The final full-scale experiments were performed with the same hydrofoil section as used in the preliminary runs, and with $d = 0{\cdot}21$ m and $\alpha = 15°$ (see figure 1). The value of d and of the cross-sectional dimensions of the hydrofoil were made smaller with a factor 2 in the half-scale experiment. The undisturbed flow depth was the same in both runs. The mean velocity in the half-scale experiment should have been a factor $2^{-\frac{1}{2}}$ of its full-scale value for Froude similarity, but its actual value deviated somewhat from this due to an inadvertent maladjustment of the controls for the discharge.

A resume of the independent experimental variables is given in table 1, in which U is the upstream cross-sectional mean flow velocity, and c and Δ are the chord and maximum thickness of the hydrofoil.

The analysis of the data, to be given in the following sections, concentrates on the velocities as the most important dependent variables. Here we list only one geometric dependent variable, namely the total variation in free surface elevation induced by the hydrofoil, which can also be considered as a measure of the breaker height H. This value was about 8 cm in the full-scale run, and about half that much in the half-scale run.

2.2. *Velocity measurements*

Velocities were measured by means of a laser–doppler velocity (LDV) meter. Such meter works on the principle of measuring the Doppler frequency shift of a laser beam scattered by small particles in a moving fluid. It measures some average velocity value in a volume with a characteristic linear dimension of the order of 1 mm. In what follows these dimensions are ignored, and we shall refer to the measurements as 'point' measurements.

In this experiment, a system was used which operates in the reference beam mode (Oldengarm 1975). A basic element in this arrangement is a rotating radial diffraction grating which functions both as a beam splitter and as a frequency shifter. The diffraction grating divides an incident laser beam into one non-diffracted zeroth-order beam and pairs of higher-order diffracted beams.

The Doppler frequency shift Δf of the scattered beam is given by

$$\Delta f = \frac{2 \sin \frac{1}{2}\phi}{\lambda} v, \tag{1}$$

in which ϕ is the acute angle between the first-order and zeroth-order beam, λ the wavelength of the laser beam, and v the fluid velocity component in the plane of the beams, normal to the bisector of the angle ϕ.

The frequency shift is measured by a frequency tracker and converted to a voltage (V). The relationship between the output voltage of the frequency tracker and the flow velocity component v is

$$v = C(V - V_0), \tag{2}$$

in which V_0 is the output voltage for zero velocity, and C is a constant which for the system used in these experiments has the value 0·263 (cm s^{-1}) mV^{-1}.

If no light scattering is detected by the laser–doppler system, the output signal contains no information about the flow velocity. This situation is called 'signal drop-out'. In this experiment, signal drop-out is most often induced by air bubble interruption of the laser beam near the breaking surface.

During signal drop-out, the frequency tracker used in this experiment keeps the output voltage the same as the voltage just before the drop-out. This is called track-and-hold operation. (In the so-called track-and-reset mode, the voltage during drop-out is made zero.) To know whether the signal drops out or not, a so-called drop-out signal is recorded simultaneously with the output of the regular channels. Such drop-out signal takes a certain constant, non-zero voltage when no signal drop-out occurs, and zero voltage during a signal drop-out. The occurrence of drop-outs was accounted for in the data analysis, as described in the appendix.

The LDV system used consists of a device radiating three beams (the zeroth-order beam and two first-order beams) and two beam detectors, so that it could measure two orthogonal velocity components simultaneously. It was so aligned that it measured the horizontal velocity (u, positive downstream) and the vertical velocity (w, positive upward) directly.

The laser beams were transmitted transversely through the flume (through the glass-panelled side-walls) and the water in it. The components radiating and detecting the signals were mounted in a fairly rigid steel frame over the flume, to maintain proper alignment. This frame could be moved in its entirety, along the flume as well as vertically.

Two outputs from the tracker corresponding to the horizontal and vertical velocities and two drop-out signals corresponding to these two outputs were recorded simultaneously in an analog magnetic tape recorder (Bell and Howell adr 1000). The recording time was 2 minutes per measurement point.

2.3. *Data analysis*

The velocity data (u, w) were separated in their time-mean values $(\overline{u}, \overline{w})$ and in fluctuations $(u', w') = (u-\overline{u}, w-\overline{w})$. The velocity fluctuations in turn were analysed to obtain r.m.s. values and mean cross-product, and in some points also the power spectrum. Most of these analyses were carried out with analog equipment, as described in the following.

Time mean velocity. A low-pass filter (cut-off frequency $f_c = 0{\cdot}05$ Hz) was used to measure the time mean velocities. After input of the signal, the output from the filter has transient oscillations around the final value. In the actual analysis, the signal of 2 min length was inputted to the low-pass filter. The first transient part of the output of 30 s length was neglected, and the remaining part of 90 s length was read and averaged to obtain an estimate of the mean velocity. This has no bias due to signal drop-outs (see the appendix).

Turbulent intensity. As shown in the appendix, the track-and-hold system provides an unbiased value for the r.m.s. of the output voltage. Therefore, the output from the LDV system can be used directly to measure the turbulent intensities.

An r.m.s. voltmeter (Thermo System, Model 1060) was used to measure the r.m.s. values of two fluctuating components. The time constants for averaging was 30 s. In this case the response of the meter is down about 10 % at 0·3 Hz. It is necessary to wait at least 3 time constants (in this case 90 s) for a reading within 2 % of the final value. In the actual analysis, the signal of 2 min length was inputted to the meter, and the output from the meter after 2 min was read to obtain estimates of u'_{rms} and w'_{rms}.

Cross product of two fluctuating velocity components. As mentioned in the appendix, the track-and-hold system gives a biased estimate of the mean cross-product in general. On the other hand, an unbiased estimate of the mean cross-product can be obtained through the track-and-reset operation, but this procedure is rather elaborate. It has been applied in parts of the data analysis, but its use was abandoned after it appeared that the simpler direct estimate from the track-and-hold system was good within an estimated 10 %.

The calculation of the cross-product $\overline{u'w'}$ was done with a small real-time computer (Hewlett and Packard, Correlator Model 3721A). The sampling interval and the record length were 0·02 s and 82 s respectively.

Power spectral density. The autocorrelation function of the track-and-hold output differs from that of the actual velocity (see appendix). The latter can nevertheless be estimated through the use of a combination of the track-and-hold signal and the drop-out signal, as shown in the appendix. This method has been applied (equation (A 5)). The required autocorrelation functions were calculated with the same correlator, sampling interval and record length as in the calculation of the mean cross-product $\overline{u'w'}$. The maximum time lag was 1·0 s. The power spectral density was calculated by digital cosine transformation of the autocorrelation function (Blackman & Tukey 1958) on an IBM 370/158 of the Delft University of Technology.

Error estimate. Systematic and random errors in the results for mean velocities and r.m.s. values were estimated from instrument specifications and reproducibility tests. The results indicated estimated relative standard errors not exceeding 10 %, except in the case of the estimated mean vertical velocity, which is sensitive to a possible

mis-alignment of the LDV system (about 2 cm s^{-1} per degree) because of the relatively large horizontal mean velocity. However, mean vertical velocities are not considered in the following, while the effect on the other results of a possible mis-alignment of even a few degrees is insignificant, as follows from calculations involving a co-ordinate axes rotation.

3. Results

Measurements of (u, w) have been made in a number of points in the central verticals of flume cross-sections at various distances (x) downstream of the centre of the hydrofoil. The minimum distance used was $x = 0{\cdot}33$ m, in the cross-section of the toe of the breaker (figure 1). The maximum distance was 4 m. It was believed that beyond that too much bottom influence would occur. Measurements were also made in the undisturbed flow, i.e. in absence of the hydrofoil.

A number of points in each vertical were used, with a height (z) above the flume bottom varying from 0·21 m (the minimum possible with the frame supporting the LDV apparatus) to somewhat below the free surface, where the signal drop-outs were judged to become too severe.

The results have been plotted in two ways, namely as a sequence of vertical profiles, and as isolines in the x, z-plane. For brevity, only the profiles of $\overline{u}$, u'_{rms} and $\overline{u'w'}$ are given here (figures 2, 3 and 4), as well as isolines of $\overline{u'w'}$ (figure 5). Some power spectra $P_{u'}(f)$ are also presented (figure 6). The results for $\overline{w}$ are not shown for the reason stated above, while those for w'_{rms} and $P_{w'}(f)$ are roughly similar to the corresponding quantities for u', except for a somewhat smaller intensity.

Data points of the full-scale experiment are indicated by crosses, and those of the half-scale experiment by open circles. The latter points have been scaled up from the measured values. The lengths have been multiplied with a factor 2. With a strict Froude scaling, the velocities should have been multiplied with a factor $2^{\frac{1}{2}}$. In fact, the ratio of the actually measured upstream mean velocities was used, which was about 1·64.

The full-scale data points have been connected by full-drawn straight-line segments for purposes of visualization.

The dashed lines $z = \text{const.}$ in the figures 2, 3 and 4 indicate the level of the centre of the hydrofoil.

4. Discussion

4.1. *General trends*

Undisturbed flow. The profiles in the lower right-hand corner of the figures 2, 3 and 4 represent flow conditions in absence of the hydrofoil. It can be seen that the mean-velocity profile is virtually uniform in the interval of the measurements (figure 2), while the turbulent shear stresses there do not deviate visibly from zero, when drawn on the same scale as the profiles for the flow with a hydrofoil (figure 4). This indicates that any influence of the bottom boundary layer on the flow in the upper flow region is insignificant compared to the dynamics of the breaking.

It is noted that the average value of $\overline{u}$ in the measurement points is about 1·35 m s^{-1} in absence of the hydrofoil (figure 2). This value is representative of the velocities in

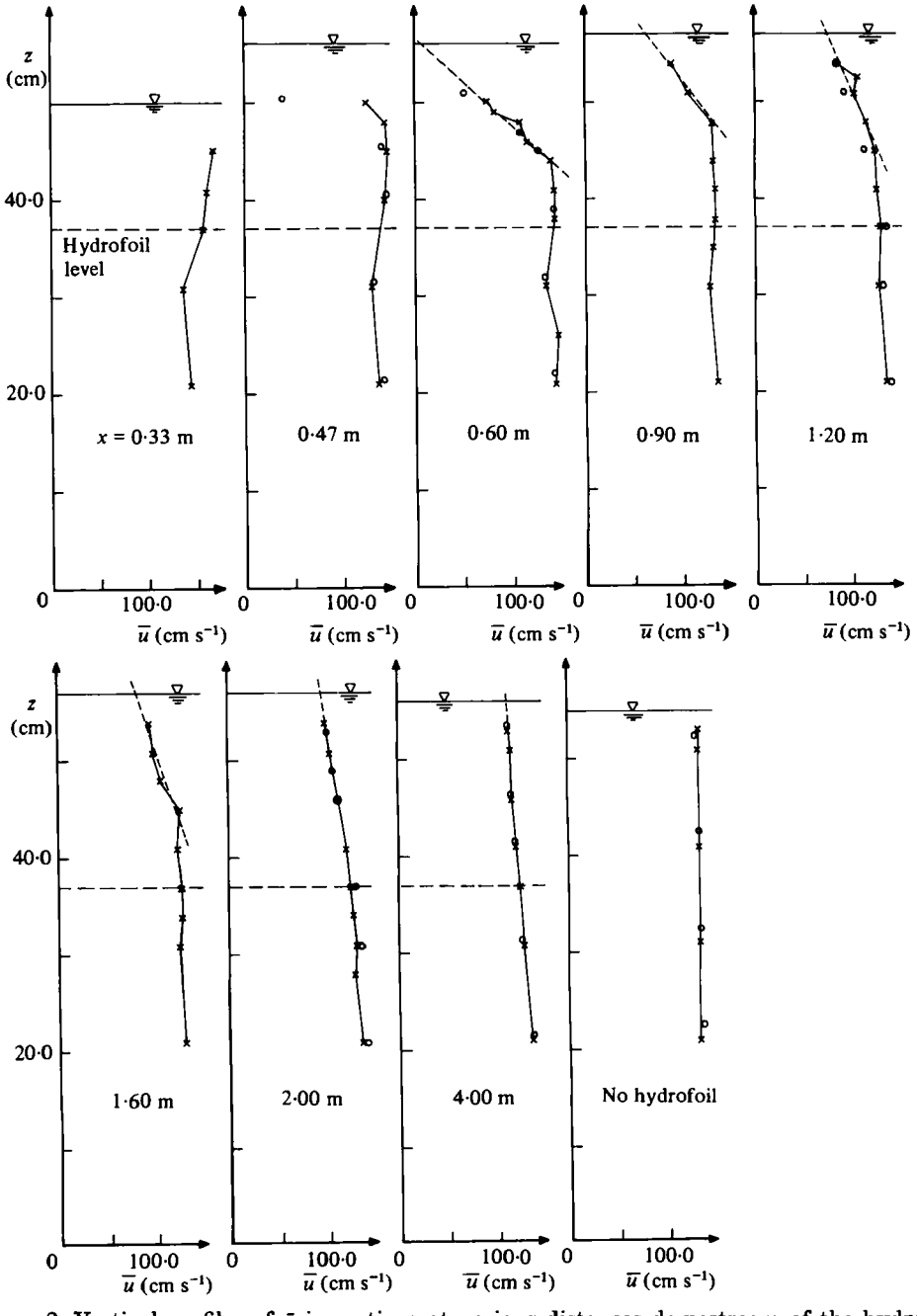

FIGURE 2. Vertical profiles of $\bar{u}$ in sections at various distances downstream of the hydrofoil. The dashed lines in the upper part indicate linear extrapolations. The profile in the lower right-hand corner is for the flow in absence of a hydrofoil. ×, full-scale experiment; ○, half-scale experiment.

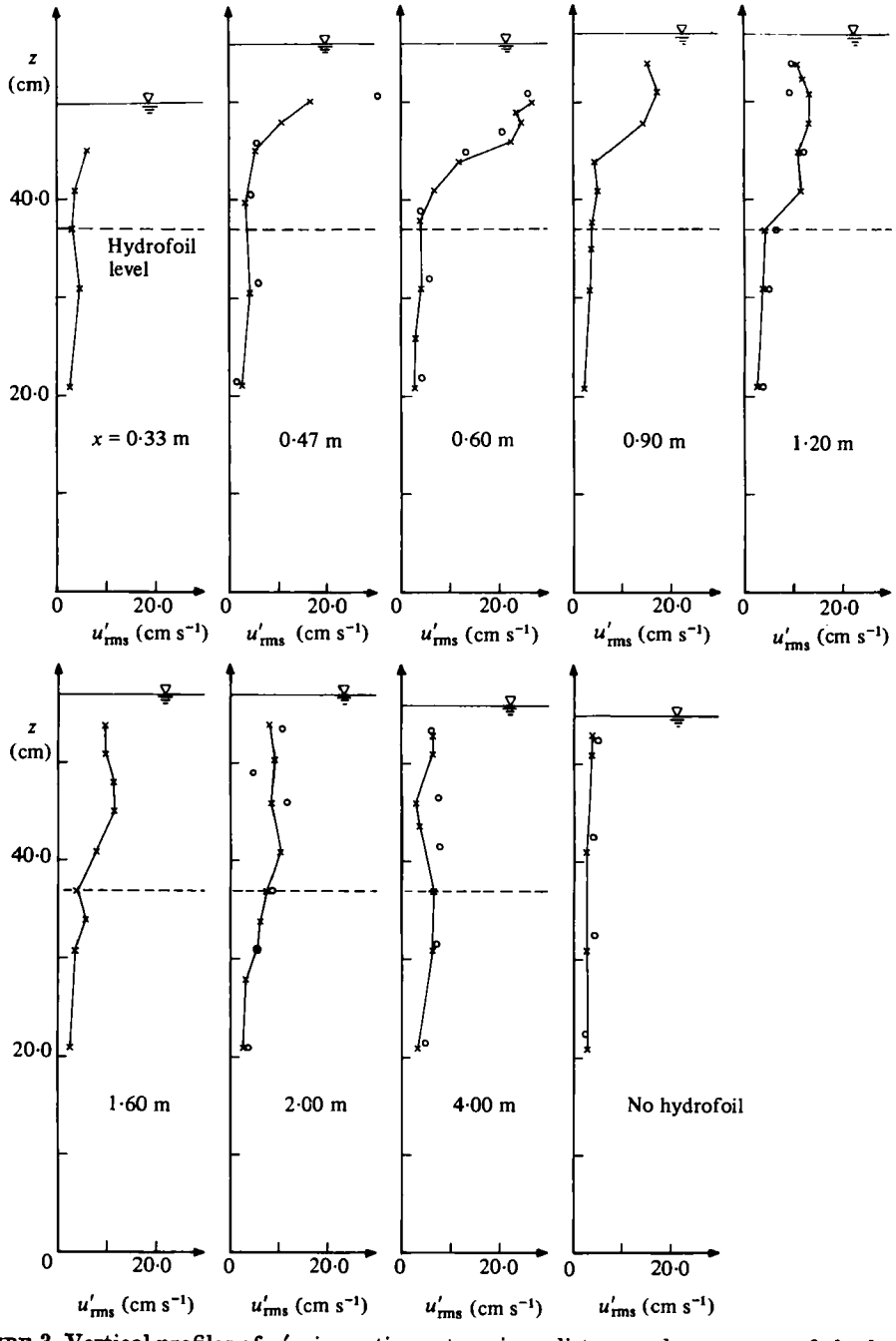

FIGURE 3. Vertical profiles of u'_{rms} in sections at various distances downstream of the hydrofoil. The profile in the lower right-hand corner is for the flow in absence of a hydrofoil. ×, full-scale experiment; ○, half-scale experiment.

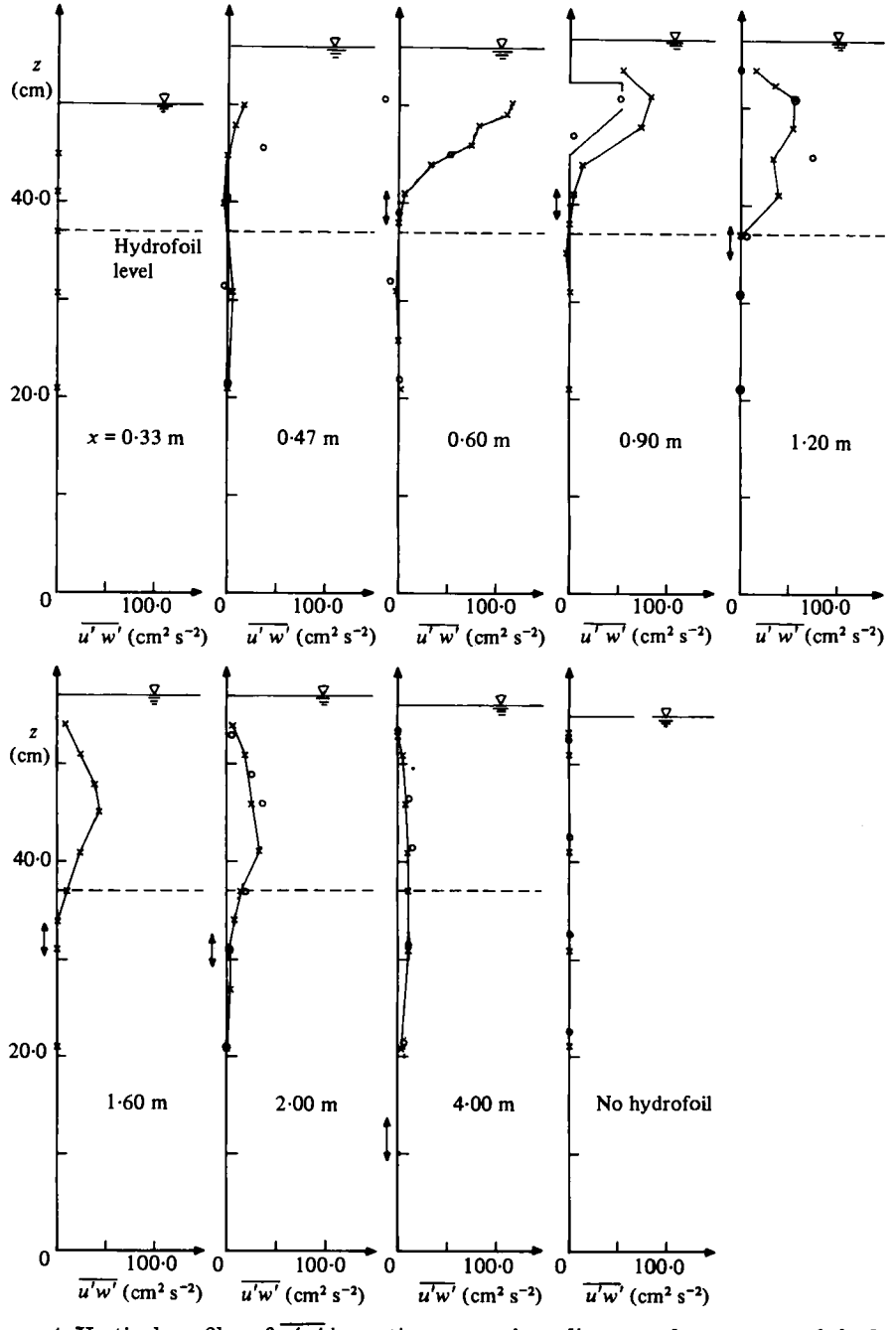

FIGURE 4. Vertical profiles of $\overline{u'w'}$ in sections at various distances downstream of the hydrofoil. The profile in the lower right-hand corner is for the flow in absence of a hydrofoil. ×, full-scale experiment; ○, half-scale experiment.

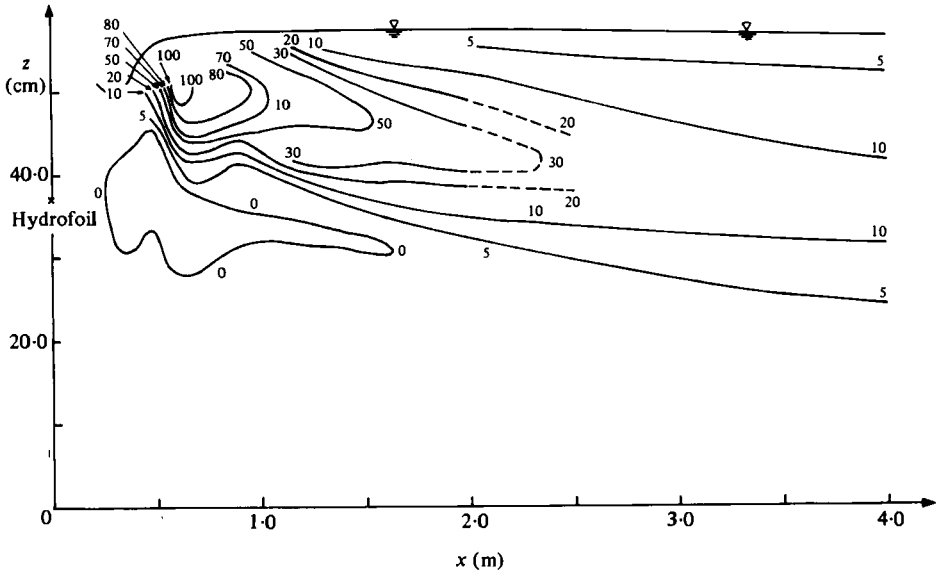

FIGURE 5. Lines of constant $\overline{u'w'}$ values downstream of the hydrofoil.

the upper part of the central vertical in a cross section. It is larger than the cross-sectionally averaged flow velocity, due to resistance of the solid boundaries. The excess is about 20 %.

Scale effects. Inspection of the figures 2, 3 and 4 shows that two regions can be distinguished as far as the similarity of the full-scale results and the half-scale results is concerned. In the most upstream region, to about $x = 0{\cdot}60$ m, significant deviations between the two sets of results occur, whereas this is not the case for the region downstream from about $x = 0{\cdot}6$ m.

The observation that similarity does seem to exist in the downstream region, despite the fact that it does not in the upstream region, proves that certain details of the flow in the region of the initial breaking are not preserved as the flow evolves downstream. This suggests the possibility of the establishment of a self-similar flow in the downstream region. This possibility will be examined in §4.2.

Mean velocity. It is clear from figure 2 that the profiles of $\bar{u}$ in the presence of the hydrofoil exhibit a strong defect near the breaking surface. This defect penetrates into the deeper region of the flow with increasing distance downstream, while at the same time it diminishes in magnitude. However, even at $x = 4$ m it is still clearly present, as can be seen by comparing that profile with the one for the flow in absence of the hydrofoil.

At the most upstream cross-sections, a slight velocity defect can be discerned at a height $z \simeq 0{\cdot}3$ m, which is an indication of the wake generated behind the hydrofoil.

It can be seen in figure 2 that the mean flow velocities beneath the surface shear layer do not vary quite monotonically with downstream distance. For instance, the velocities at $x = 0{\cdot}60$ m are slightly in excess of those at $x = 0{\cdot}47$ m and at $x = 0{\cdot}90$ m. This observation could indicate an undular flow in that region, but that has not been confirmed by direct measurements of the dividing streamlines. In the region immediately following the breaking, the mean free surface itself cannot *a priori* be

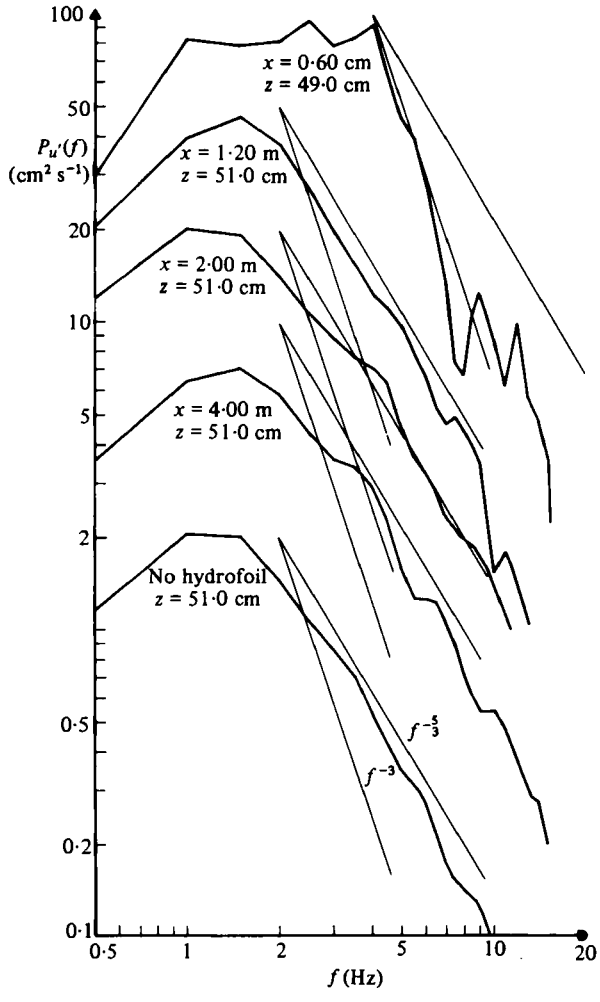

FIGURE 6. Power spectra of u' in four points within the shear layer induced by the breaking, and in one point at the same elevation in the undisturbed flow. The straight lines indicate variations $\sim f^{-3}$ and $\sim f^{-\frac{5}{3}}$.

taken to be the upper dividing streamline for the main flow, because of a possible surface roller. A precise determination of the location of the dividing streamline by means of dye injection is impossible because of the rapid mixing, whereas the LDV system could not be used there because of the aeration.

Turbulence intensity. Figure 3 shows that the turbulence has its greatest intensity near the toe of the breaking surface, from where it decays downward and downstream. At $x = 4$ m, the station farthest downstream, it is still significantly in excess of its value in the undisturbed flow. The wake of the hydrofoil shows up in figure 3 as a slight excess of u'_{rms}.

In figure 6 power spectra of u' are presented for a number of points at various distances downstream, at a height of about 0·5 m above the flume bottom, that is within the turbulent layer induced by the breaking. A spectrum for the undisturbed flow is also shown. Inspection of figure 6 shows that the spectra are more or less similar in

form, with the exception of the spectrum at the most upstream point ($x = 0{\cdot}6$ m). The latter has a high-frequency tail of about f^{-3}, while the others vary more nearly as $f^{-\frac{5}{3}}$ (which is characteristic for the inertial-advective subrange in turbulence spectra; Tennekes & Lumley 1977). The mutual similarity of the downstream spectra, and their being different in form from the upstream spectrum at $x = 0{\cdot}6$ m, indicates a loss of local details and a tendency towards some more universal form as the flow evolves downstream, which was also noted in the discussion of scale effects.

Reynolds stress. The quantity $\overline{u'w'}$, which is proportional to the Reynolds shear stress, has significant non-zero values only in a fairly well-defined upper layer downstream of the toe of the breaker (figures 4 and 5). It is virtually zero in the cross-section of this toe ($x \simeq 0{\cdot}33$ m); no evidence of a wake behind the hydrofoil is present in this profile.

4.2. *Comparison with self-similar shear flows*

The preceding discussions of scale effects and of the power spectra of u' have given an indication that the flow downstream from the region of the initial breaking tends to a self-similar form. In the classical theory of turbulence a number of freely evolving shear flows has been studied, such as mixing layers, jets and wakes, assuming self-similarity. In this section, the question will be considered to which extent the observed flow corresponds to one of these.

A mixing layer forms the transition between two uniform parallel flows of different mean velocity, while a jet and a wake can be seen as laterally limited regions of velocity surplus and velocity deficit, respectively, relative to the undisturbed flow. In a mixing layer the cross-stream variation in mean flow velocity is constant in the downstream direction (if the two external flows have a sufficient lateral dimension), while this quantity decreases downstream in jets and wakes.

It follows from the above that the flow observed in our experiment, which is characterized by having a velocity deficit with respect to the undisturbed flow, which deficit is decreasing downstream, is qualitatively most nearly like a flow in a wake. This can be checked quantitatively, or at least semi-quantitatively, by estimating the values of some characteristic parameters and their variation downstream, and comparing these with the corresponding results for a typical wake flow. This is done in the following.

The quantities to be considered in the comparison are the mean velocity defect ($\overline{u}_d$), a characteristic value for the turbulent velocity magnitude ($\tilde{u}'$), and a lateral length scale (l).

Asymptotic theoretical relations have previously been derived between these quantities and their variations downstream, for a variety of shear flows, assuming a high Reynolds number (Re) and a nearly parallel, self-preserving flow, away from bounding surfaces. The results are asymptotic in the sense of $Re^{\frac{1}{2}} \gg 1$ and $l \ll L$, in which L is a longitudinal length scale, as well as in the sense that only the far field is considered, sufficiently far downstream from the physical origin of the shear layer, so that the flow has settled down to self-preservation. The results for a plane wake are (cf. Tennekes & Lumley 1977):

$$\tilde{u}' \propto \overline{u}_d \propto x_*^{-\frac{1}{2}}, \quad l \propto x_*^{\frac{1}{2}};$$

$x_* = x - x_0$ is the distance downstream from a reference point $x = x_0$.

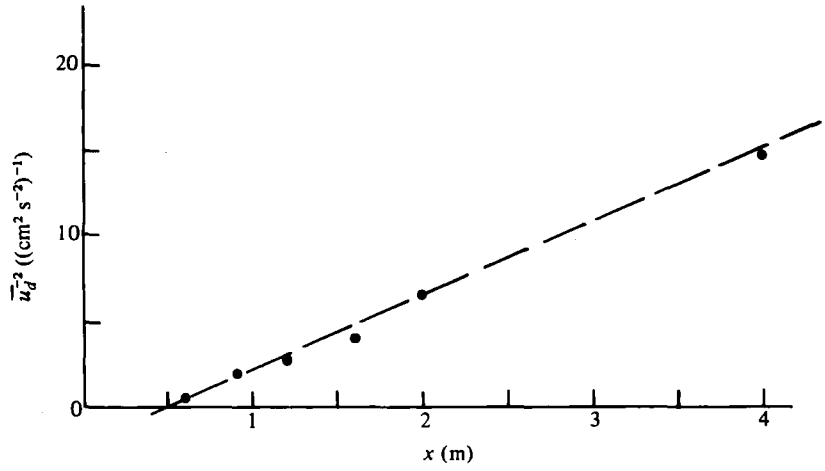

FIGURE 7. Variation of $(\bar{u}_d)^{-2}$ with x, the distance downstream from the hydrofoil. A straight line has been fitted to the data points (●) by eye.

Experimental values of $\bar{u}_d$, $\tilde{u}'$ and l were determined as follows. The mean velocity defect was calculated as $\bar{u}_d = \bar{u}_l - \bar{u}_f$, in which $\bar{u}_l$ is the value of $\bar{u}$ in the lowest point of measurement ($z = 0{\cdot}21$ m), and $\bar{u}_f$ the value of $\bar{u}$ at the mean free surface elevation, as estimated by linear extrapolation of the upper part of the measured profile (see the dashed lines in figure 2). For $\tilde{u}'$ the maximum value of u'_{rms} in the vertical profile was taken, and l was defined as the width of the shear layer, from the mean free surface elevation down to the fairly abrupt transition between the region of high shear above and the more or less homogeneous flow beneath. The locations of these transition zones were estimated from the vertical distributions of $\overline{u'w'}$; they have been indicated in figure 4 by vertical arrows.

The most upstream cross-sections where meaningful estimates could be made were $x = 0{\cdot}60$ m for $\bar{u}_d$ and l, and $x = 0{\cdot}90$ m for $\tilde{u}'$ (see figures 2, 3 and 4).

For a comparison of the observed downstream variations of $\bar{u}_d$, $\tilde{u}'$ and l with the theoretical ones, it is necessary to have an estimate of the location of the reference point $x = x_0$. A theory for self-preserving flow cannot predict this location in terms of the details (local length scales) of the physical origin of the flow, since by definition a self-preserving flow has no 'memory' of those details. In the present case, the physical origin of the wake flow may be taken to be near the cross-section of initial breaking, $x = x_b \simeq 0{\cdot}33$ m (see figure 1), and the jump height H can be taken as a characteristic length scale for the initial wake flow. Thus, all one can say *a priori* about the point $x = x_0$ is that it should be near $x = x_b$, to within a distance of order H, or $x_0 = x_b + O(H)$. If one considers points far downstream ($x - x_0 \gg H$) then it is of course immaterial whether $x_0 = x_b$ exactly or $x_0 = x_b + O(H)$, but since our measurement points do not necessarily fulfil this condition we must allow x_0 to differ from x_b.

An estimate of $(x_0 - x_b)$ can be obtained from the measurements, by optimizing in some sense the fit of the data to some theoretical model. To this end, an auxiliary plot was made of $(\bar{u}_d)^{-2}$ *vs.* x on linear scales (figure 7). A straight line was fitted to the data points by eye. The intercept of this line with the level $(\bar{u}_d)^{-2} = 0$ provides

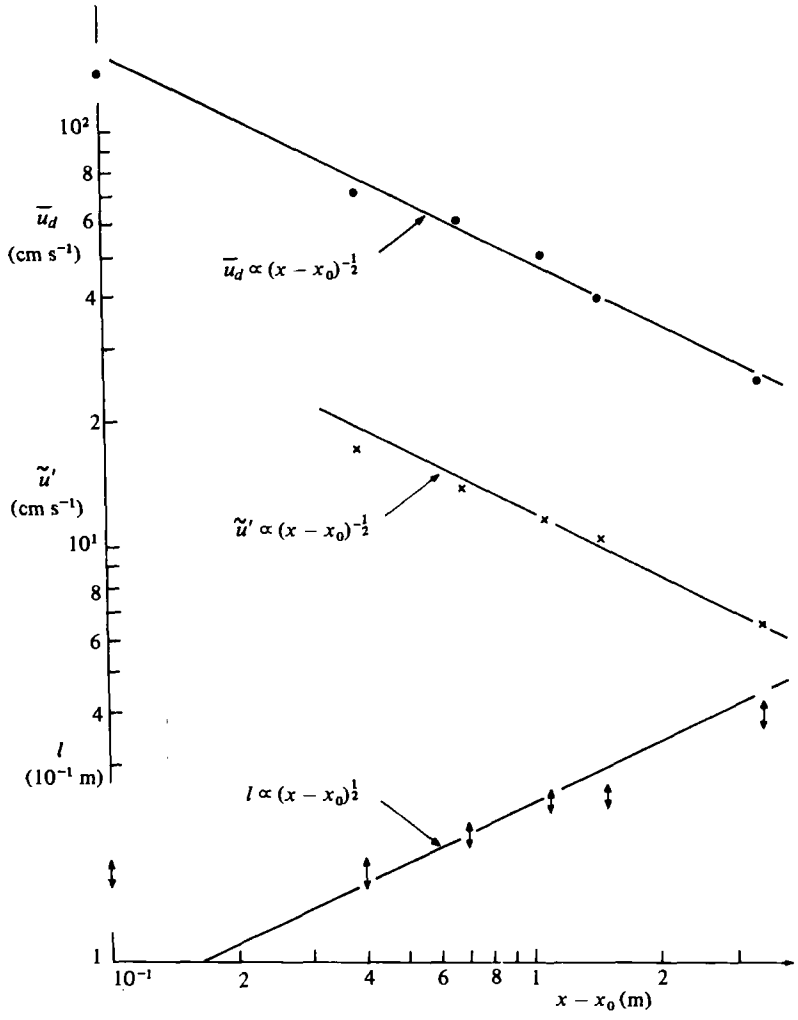

FIGURE 8. Variation of flow parameters with x_*, the distance downstream from the reference point $x = x_0$, for $x_0 = 0{\cdot}5$ m. Mean velocity defect (●), turbulent intensity (×) and layer thickness (↕). The straight lines indicate proportionalities to $x_*^{\pm\frac{1}{2}}$.

an estimate $x_0 \simeq 0{\cdot}5$ m. (This gives $x_0 - x_b \simeq 0{\cdot}17$ m $\simeq 2H$, consistent with the order-of-magnitude estimate given above.)

The variations of $\bar{u}_d$, $\tilde{u}'$ and l with the downstream distance x_*, using $x_0 = 0{\cdot}5$ m, is shown on log–log scale in figure 8. Straight lines $\sim x_*^{\frac{1}{2}}$ and $\sim x_*^{-\frac{1}{2}}$ have been added for reference. It appears that $\bar{u}_d$ and $\tilde{u}'$ both vary with x_* approximately as $x_*^{-\frac{1}{2}}$, as in plane wake. The mean trend of l with x_* in the range $x_* \geqslant 0{\cdot}4$ m is approximately $l \sim x_*^{0{\cdot}4}$, but the results are not inconsistent with $l \sim x_*^{\frac{1}{2}}$, considering the uncertainty in the estimate of l. (A quantification of this uncertainty in terms of significance levels is not given because that in itself is too uncertain, in view of the subjective manner in which l has been determined in figure 4.) On the whole, we conclude that the flow downstream of the breaking surface is not only like a wake flow in a qualitative sense, but also in a more quantitative sense.

5. Conclusions

Measurements have been made of horizontal and vertical velocities, including turbulent fluctuations, in a steady mean flow with a breaking surface, similar to a so-called spilling breaker in shallow water. These measurements have given rise to the following conclusions:

(1) A region downstream of the initiation of breaking can be recognized in which the flow evolves as in a free self-preserving turbulent wake. This conclusion rests on the observed downstream variation of mean velocity defect, turbulence intensity and shear-layer thickness.

(2) The measurements of the flow in the region mentioned in conclusion (1) appear to be free of scale effects if scaled up according to Froude's law.

The authors thank Dr D. H. Peregrine for helpful discussions and suggestions. One of us (T. S.) thanks the Delft University of Technology for granting him a Research Fellowship.

Appendix. Effect of signal drop-out on parameter estimation

Let $u(t)$ denote the output signal of a channel of the LDV system which would be obtained if there were no signal drop-outs. In the so-called track-and-hold mode, the system gives as output during each drop-out interval the signal value of the instant immediately preceding the drop-out. Let $(t_i, t_i + T_i)$ denote the time interval during which the ith drop-out occurs. The output $y(t)$ in the track-and-hold mode can then be written as

$$\begin{aligned} y(t) &= u(t_i) \quad \text{for} \quad t \in (t_i, t_i + T_i) \\ &= u(t) \quad \text{for} \quad t \notin (t_i, t_i + T_i), \quad i = 1, 2, \ldots . \end{aligned} \tag{A 1}$$

We define an auxiliary signal, the so-called drop-out signal, by

$$\begin{aligned} d(t) &= 0 \quad \text{for} \quad t \in (t_i, t_i + T_i) \\ &= 1 \quad \text{for} \quad t \notin (t_i, t_i + T_i), \quad i = 1, 2, \ldots . \end{aligned} \tag{A 2}$$

The signals $u(t)$, $y(t)$ and $d(t)$ will be considered as realizations of stationary stochastic processes $\{\mathbf{u}_t\}$, $\{\mathbf{y}_t\}$ and $\{\mathbf{d}_t\}$, respectively. Information about $\{\mathbf{u}(t)\}$ has to be recovered from samples of $y(t)$ and $d(t)$, which have been recorded.

It is normally assumed (cf. Oldengarm 1973; Buchhave, George & Lumley 1979) that the random occurrences of drop-outs are independent of the instantaneous velocity in the measurement volume. In the present experiments, most if not all drop-outs are caused by the presence of one or more air bubbles in the optical path of the LDV system. Since air bubbles are entrained at the surface, the velocity of the water around it may have a bias toward the surface values. This in turn could imply a correlation of drop-out occurrences with the velocity. However, this effect decreases with increasing residence time of the bubble in the water, due to the loss of (Langrangian) correlation of the instantaneous local water velocity with the velocity at the time of entrainment, and also because of the relative motion between bubble and water. In any event, possible effects of correlation between drop-out occurrence and velocity are neglected in the following analysis. On this assumption, the values of $\mathbf{u}_t$

at the instants when a drop-out begins ($\mathbf{u}_{t_i}$) have the same probability distribution as $\mathbf{u}_t$ for arbitrary t. It follows, in view of (A 1), that $\mathbf{y}_t$ and $\mathbf{u}_t$ are identically distributed, and thus that they have the same mean, mean square, and so on.

The preceding result applies to parameters of the single variable $\mathbf{u}_t$, with a one-dimensional probability distribution. It is not necessarily valid for the joint statistics of $(\mathbf{u}_{t_1}, \mathbf{u}_{t_2}, \ldots)$ at two or more different times, or two or more outputs $(\mathbf{u}_t, \mathbf{v}_t, \ldots)$. On the contrary, it has been shown (Oldengarm 1973; Buchhave *et al.* 1979)† that in general $R_y(\tau) \neq R_u(\tau)$ for $\tau \neq 0$, in which $R_y(\tau) = E\{\mathbf{y}_t \mathbf{y}_{t+\tau}\}$ is the autocorrelation function of $\mathbf{y}_t$, and likewise for R_u, and that $E\{\mathbf{y}_t^{(1)} \mathbf{y}_t^{(2)}\} \neq E\{\mathbf{u}_t^{(1)} \mathbf{u}_t^{(2)}\}$ in general, in which the superscripts (1) and (2) denote signals from different channels. To circumvent this problem, use can be made of the so-called track-and-reset output $r(t)$, which is zero during a drop-out, such that

$$r(t) = d(t)\, u(t) \quad \text{for all } t. \tag{A 3}$$

The autocorrelation function of the process $\{\mathbf{r}_t\}$ is

$$R_r(\tau) = E\{\mathbf{r}_t \mathbf{r}_{t+\tau}\} = E\{\mathbf{d}_t \mathbf{d}_{t+\tau} \mathbf{u}_t \mathbf{u}_{t+\tau}\} = R_d(\tau)\, R_u(\tau), \tag{A 4}$$

where use has been made of the fact that $(\mathbf{d}_t, \mathbf{d}_{t+\tau})$ are stochastically independent of $(\mathbf{u}_t, \mathbf{u}_{t+\tau})$, which in turn is a consequence of the assumption that the instants of onset of a drop-out are independent of $\mathbf{u}_t$. Therefore,

$$R_u(\tau) = R_r(\tau)/R_d(\tau). \tag{A 5}$$

The LDV system used in the present study worked in the track-and-hold mode, giving outputs $y(t)$ and $d(t)$. After using the equality $r(t) = d(t)\, y(t)$, the autocorrelation functions in the right-hand side of (A 5) can be estimated from these outputs by conventional methods. The mean unlagged product $\overline{u'w'}$ can be found in a similar manner as $R_u(\tau)$.

REFERENCES

Abbott, I. H. & Von Doenhoff, A. E. 1949 *Theory of Wing Sections*. McGraw-Hill.

Blackman, R. B. & Tukey, J. W. 1958 *The Measurement of Power Spectra*. Dover.

Burchhave, P., George, W. K. & Lumley, J. L. 1979 *Ann. Rev. Fluid Mech.* **11**, 443–503.

Führböter, A. 1970 *Proc. 12th Conf. Coastal Engng, Washington D.C.*, vol. I, pp. 391–398.

Longuet-Higgins, M. S. & Turner, J. S. 1974 *J. Fluid Mech.* **63**, 1–20.

Oldengarm, J. 1973 *TPD Information Paper*, no. 906–5.

Oldengarm, J. 1975 *Proc. LDA-Symp., Copenhagen*, pp. 553–564.

Peregrine, D. H. & Svendsen, I. A. 1978 *Proc. 16th Conf. Coastal Engng, Hamburg*, vol. 1, pp. 540–550.

Resch, F. J. & Leutheusser, H. J. 1972 *J. Hydraulic Res.* **10**, 409–430.

Resch, F. J., Leutheusser, H. J. & Coantic, M. 1976 *J. Hydraulic Res.* **14**, 293–319.

Stive, M. J. F. 1980 *Proc. 17th Conf. Coastal Engng, Sydney* (in press).

Tennekes, H. & Lumley, J. L. 1977 *A First Course in Turbulence*. Massachusetts Institute of Technology Press.

† In 2.7.12 of Burchhave *et al.*, which is an expression for $R_y(\tau)$ (in our notation), a term $R_{\bar{I}}(1-\bar{I})^2$ should be added to the right-hand side (using the notation of these authors). Apart from this, the estimate for the variance spectral density of $\mathbf{y}_t$ presented by these authors (equation (2.7.13)) is incorrect, since it is given as $P_{u'}(f)$ plus a term which is positive for all frequencies. This is in conflict with the fact that the variances of $\mathbf{y}_t$ and $\mathbf{u}_t$ have exactly the same value, which is also mentioned by Buchhave *et al.* Adding the spectrum corresponding to the above-mentioned missing term in $R_y(\tau)$ would only make the error greater, since power spectral densities are non-negative.